J. King Saud Univ., Vol. **2**, *Eng. Sci.* (2), pp. 275–293 (1410H/1990)

A Computational Method of Analysis of the Log-Periodic Dipole Antenna

Mohamed A. Hassan
Department of Electrical Engineering, College of Engineering, King Saud University, P.O.Box 800, Riyadh–11421, Saudi Arabia

Abstract. An efficient numerical method is presented here for the analysis of the log-periodic diploe antenna arrays. The log-periodic dipole array is first considered as a parallel connection of two electrically decoupled circuits, the dipole array circuit and the feeder circuit. The dipole array is then treated as a boundary value problem represented by a set of integral equations. These equations are solved through the use of Bubnov-Galerkin's matrix technique with Lagrangian interpolation polynomials as basis functions. The method permits a precise and complete evaluation of the performance of antennas operating over any given frequency band and for any given design parameters. Many diagrams are presented, for different values of the scale factor (τ), the spacing factor (σ) and the characteristic impedance of the feeder transmission line (Z_f), in order to find the best compromise among those parameters for an accurate antenna design. The results obtained show good agreement with those obtained by other investigators.

Introduction

The radiation characteristics of a single wire antenna are very sensitive to frequency. In many applications, it is necessary to design frequency independent antennas with coverage of a broad range of frequencies. These are required to meet the demand of broadband systems and to assist in the exploration and utilization of most of the electromagnetic spectrum. One of the most successful and useful broadband antennas is the log-periodic dipole antenna (LPDA), which is first developed by Isbell in 1960 [1], and whose description is given briefly in the next section.

Later, Carrel [2] presented a step-by-step procedure for the analysis of the LPDA. He assumed that the current distribution of the dipole element is sinusoidal, that the mutual impedance between any two elements is not affected by the presence of the other elements, and that the array is considered as a parallel connection of two

electrically decoupled circuits; the antenna circuit and the feeder circuit. He derived a system of equations to relate the currents at the input of the dipole elements to the current at the input terminals of the whole antenna. Two admittance matrices $[Y_a]$ and $[Y_L]$ were formulated for the solution of such a system. The first was that of an N-port network composed of N dipoles, mutually coupled to each other, while the latter being that of another N-port network, composed by the feed line with the feed points of the dipoles as its terminals.

This sinusoidal current distribution along the dipoles seemed to Cheong and King [3] to be a poor assumption. They presented a more accurate representation of the current distribution, and hence, derived a similar system of equations as that of Carrel. Also, both Carrel and Cheong and King analyses had the same $[Y_L]$ matrix, but they differed in the derivation of the elements of $[Y_a]$. Unfortunately, their theory was only applicable to dipole elements with half lengths less than 0.625λ. This restriction greatly reduced its usefulness to the analysis of arrays with bandwidth greater than 2:1. DeVito and Stracca [4] introduced some modifications on the diagrams previously presented by Carrel. They used the analysis of Cheong and King [5], in their study of linear dipole arrays with unequal lengths and unequally spaced dipoles; and considered the dipole current distribution with three symmetric sinusoidal terms. More diagrams were presented later [6] for more accurate design on the log-periodic dipole antennas including those for higher power applications.

Also, Kyle [7] calculated the mutual impedances between the dipoles based on Carrel's assumption. However, the currents were approximated by pulse functions and the numerical point matching technique [8] was then applied. In order to avoid invoking Carrel's assumption of the sinusoidal current distribution on the radiators, and for current representation more accurate than that of Cheong and King, the method of moments was also employed by Sinnott [9] to obtain accurate numerical results for the antenna performance. His approach permitted the multiple frequency analysis of the LPDA without repeating all computations at each frequency. In search for the causes of the anomalous behavior of the LPDA, Gong and Balmain [10] suggested a computer analysis for such antenna using Richmond's computer program for thin wire structures.

The work on the LPDA in free space environment has been extended to treat the LPDA array with printed circuit, microstrip or stripline geometries. In their design of a stripline-type LPDA, Campbell *et al.* [11] modified Carrel's method to include an effective relative dielectric permittivity in computations relating to dipole lengths and spacings. However, they did not deal with the feeding technique thoroughly. In an attempt to unite the requirements of high gain, broad bandwidth, low weight, reliability, ease of manufacture and integration, Pantoja *et al.* [12] pre-

sented a feeding technique of the printed planar LPDA and took into account the effect of the dielectric substrate on the antenna design. They also employed the numerical finite element method in their analysis.

Therefore, as it might be seen from the above survey, the new trend in the analysis of the LPDA is the use of computational numerical techniques. This is because of many advantages such as cost reduction, accuracy and speed. Also, one can deduce that the most attractive method for such analysis – without any restriction – is the moment method. More advantages such as stability, convergence and storage reduction, can be gained if the Bubnov-Galerkin's technique is applied.

Here, a Bubnov-Galerkin's method is developed in order to analyse the log-periodic dipole antenna and obtain complete information on the antenna performance. The LPDA is considered to be located in free space and linearly polarized. Carrel's approach is adopted to represent the LPDA by the parallel connection of an array of straight wire dipoles and a feeder transmission line. The $[Y_L]$ matrix elements of the N-port network, composed by the feed line with the N terminal pairs at the feed points of the N dipoles, are taken from [7]. However, the $[Z_a]$ (where $[Z_a]=[Y_a]^{-1}$) matrix elements of the N-port network, composed by the N-dipoles mutually coupled to each other, are derived here. This is by considering the array of dipoles as a boundary value problem and formulating a set of integral equations governing the current distribution on the dipoles [13]. By employing the Bubnov Galerkin's method [13] with polynomial approximation, the set of integral equations is transformed into a matrix equation. $[Z_a]$ elements are thus derived from the resulting generalized impedance matrix of that matrix equation. The base currents and voltages of the dipoles are hence determined. The radiation pattern, directivity, gain and input impedance are also calculated. By changing the various antenna parameters, general characteristics curves are plotted showing the antenna performance under different conditions, and allowing engineers to find the best compromise among the various parameters for the antenna design.

Problem Description

The log-periodic dipole array (LPDA) is one of the most widely used broadband antennas. It consists, as shown in Fig. 1, of a nonuniformly spaced array of N parallel linear dipoles. They all lie, in free space, in the vertical y-z plane, parallel to the z-axis and with the y-axis as the line of symmetry. The lengths ($l_i = 2h_i$, i = 1, ...N) of the dipoles, their radii (a_i, i=1, ...N), their in between spacings (d_i, i=1, ...N–1) and their distances from the apex (y_i, i=1, ...N) form a geometric progression τ, *i.e.*

$$\tau = \frac{l_n}{l_{n-1}} = \frac{a_n}{a_{n-1}} = \frac{d_n}{d_{n-1}} = \frac{y_n}{y_{n-1}}$$

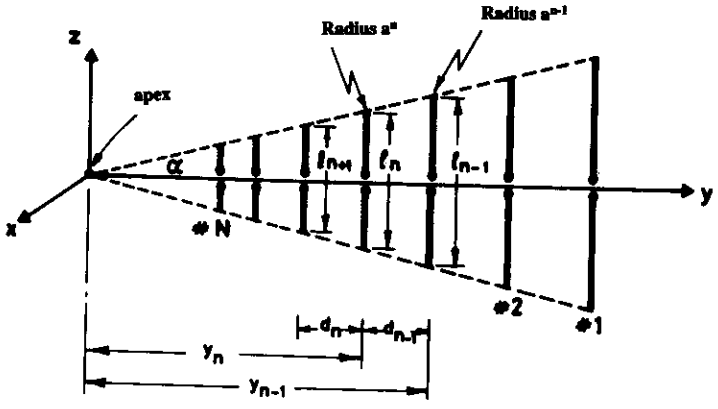

Fig. 1. Schematic configuration of the log-periodic dipole antenna

The ratio of the distance between two adjacent elements to twice the length of the larger element is known as the spacing factor σ, *i.e.*

$$\sigma = \frac{d_{n-1}}{2\,l_{n-1}} = \frac{d_n}{2\,l_n} = \frac{1-\tau}{4}\cot\alpha$$

where α is the angle, at the apex, between the line joining the ends of the dipole elements and the center line.

The dipoles are fed at their centers by a parallel-wire transmission line of characteristic impedance Z_f, and terminated by an impedance Z_T at a distance s from the large element side. On the smallest element side, the antenna is driven by a generator. This generator feeds the dipoles, through the transmission line, in an alternating fashion and introduces a phase shift of 180° from element to element in addition to that due to the electrical length of line between them. This mechanical phase reversal of the alternate elements is necessary for the antenna to exhibit a broadband performance.

It is worthwhile to give, at this point, a brief description of the operation of the LPDA antenna. It may be divided into three main regions. The active region consists of several dipoles whose lengths are around half-wavelength. This means that they are nearly resonant at a particular operating frequency, and hence their current magnitudes are relatively large. On one side of the active region, there exists the reflection region with dipoles larger than the half-wavelength at that frequency; while on the other side, a group of elements smaller than half-wavelength forms the transmis-

sion region. The dipole currents in both these regions are relatively small. Therefore, at each frequency, only a small portion of the antenna (*i.e.* the active region) radiates. And, it may be concluded that at the lower frequency limit of the operating bandwidth, the active region includes the largest element, and it moves from one group of elements to another until it includes the shortest element at the upper frequency limit. The structural bandwidth B_s is defined to be the ratio of the lengths of the largest to the smallest dipole element.

Solution of the Log-Periodic Dipole Array Problem

If the small coupling between the feeder and the antenna elements is neglected, then the LPDA structure may be approximated by an equivalent circuit composed of the parallel connection of two decoupled circuits, the feeder circuit and the antenna circuit [2]. The first circuit, Fig. 2, consists of the feeder with alternating terminals to which the dipole elements are eventually attached. This circuit is represented by the matrix equation,

$$[\,I_L\,] \;=\; [\,Y_L\,][\,V_L\,] \tag{1}$$

where $[I_L]$ is a column vector whose entries are the N driving currents of the feeder circuit, and $[V_L]$ is also a column vector with N driving voltages at the N ports. $[Y_L]$ is the short circuit admittance matrix of the feeder N-port network. The entries of $[Y_L]$ are taken here as defined in [7].

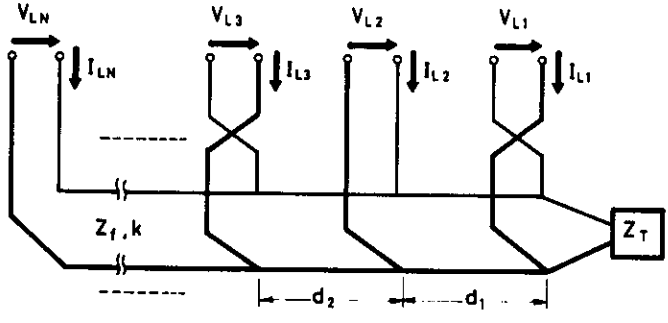

Fig. 2. The feeder circuit of the equivalent circuit for the LPDA

The fields of the dipole elements determine the driving-point impedances of the elements, which shunt the feeder. The circuit properties of the elements are described by an N terminal pair circuit. This antenna circuit can be represented by,

$$[\,Z_a\,][\,I_a\,] \;=\; [\,V_a\,] \tag{2}$$

where $[I_a]$ and $[V_a]$ are the column vectors whose entries are respectively the driving base currents and voltages of the antenna circuit. $[Z_a]$ is the impedance matrix of the antenna circuit with its entries to be determined, here, by a newly developed technique presented in the next section.

Now, by connecting both circuits in parallel, the overall LPDA circuit is thus represented by

$$[I_L] + [I_a] = [I] \tag{3}$$

where [I] is the vector of the input driving currents externally fed to the LPDA. As the LPDA is only fed across the smallest dipole element, therefore the entries of vector [I] are all zeros except its N^{th} entry. It is set equal to 1 Ampere. Thus,

$$[I] = [000....1]^T \tag{4}$$

Substitution from (1) and (2) into (3), we obtain

$$[Y_L][V_L] + [Z_a]^{-1}[V_a] = [I] \tag{5}$$

but, we have

$$[V_L] = [V_a] \tag{6}$$

Therefore upon substitution of (6) into (5) we, obtain

$$\{[Y_L] + [Z_a]^{-1}\}[V_a] = [I] \tag{7}$$

Equation (7) is the matrix equation of the LPDA structure which gives, upon its solution, the base voltage vector $(V_a]$ of the antenna dipoles. Now, since $[Y_L]$ has already been defined elsewhere [7], and [I] is given by (4), the problem now reduces to finding the inverse of the antenna impedance matix $[Z_a]^{-1}$. Once, equation (7) is solved for $[V_a]$, the driving currents at the base of the antenna, represented by $[I_a]$, is found from (2). The input impedance, calculated at the junction between the feeder and the smallest dipole element, is thus given by the ratio of the base voltage across the N^{th} dipole element to the base current fed to that element.

Determination of the Impedance Matrix of the Antenna Circuit

The dipoles of the antenna circuit are considered, as shown in Fig. 1, as an array of N nonuniformly separated dipoles of different lengths and different radii. At the upper frequency of the bandwidth (*i.e.* when the shortest dipole near the generator is half-wavelength long) the largest dipole is of course longer than half-wavelength. It becomes longer and longer in terms of the wavelength of the highest frequency as

the structural bandwidth increases. In order to have moderate wire sizes to deal with later, each dipole is divided into two wire segments or more connected together. Therefore, the dipole array problem is reduced to solving that of an antenna structure of M wire segments, say.

For this new antenna configuration, M electric field integral equations are formulated. Each wire segment is represented by a single integral equation with the current distribution on the wire as unknown under the integral sign. These equations are obtained by applying the boundary condition requiring that the tangential electric field on each and every element is zero. Similar equations are obtained in a previous research work dealing with wire scatterers [13],

$$\frac{1}{4\pi j\omega\varepsilon}\sum_{m=1}^{M}\int_{0}^{l_m} I^m(s_m)\,F(s_n, s_m)\,ds_m + \hat{z}.\bar{E}_n^{i_m}(s_n) = 0 \qquad ;n = 1,2,\ldots M \tag{8}$$

where $I^m(s_m)$ is the current at the source point s_m on wire element m whose length is l_m and $F(s_n, s_m)$ is (as derived in the appendix),

$$F(s_n, s_m) = \frac{\exp(-jkR_{mn})}{R_{mn}^5}\left[R_{mn}^2(-1-jkR_{mn} + k^2R^2_{mn}) + (z_n - z_m + s_n - s_m)^2\,(3 + j3kR_{mn} - k^2R^2_{mn})\right] \tag{9}$$

R_{mn} is the distance between the field point s_n on wire n and the source point s_m on wire m. It is given by,

$$R_{mn}^2 = (y_n - y_m)^2 + (z_n - z_m + s_n - s_m)^2 + a_n^2 \tag{10}$$

(y_n, z_n) and (y_m, z_m) are the cartesian coordinates, in the y-z plane, of one end of wire elements n and m respectively. k is equal to 2π/wavelength. $\bar{E}_n^{i_m}(s_n)$ is the tangential component of the impressed electric field along wire n at point s_n. Simple harmonic time dependence at angular frequency ω, exp ($j\omega t$), is assumed and will be suppressed in all field quantities. ε is the permittivity of the medium. Note that the 180° phase shift due to the alternate connection of the adjacent dipoles to the transmission line is included by assuming a reversal in the conventional directions of the currents flowing in neighbouring dipoles as shown in Fig. 2. This current reversal appears as a minus sign in the mutual impedance, *i.e.* $F(s_n, s_m)$ of (9) is negated as mentioned in the appendix.

The resulting integral equations (8) are then solved through the use of Bubnov Galerkin's projective method with Lagrangian interpolation polynomials as basis functions. This will transform the system of integral equations into a set of linear algebraic equations. Also, Kirchhoff's current law is applied, at every connection between wire segments, to reduce the number of these equations by the number of joints in the structure. Therefore, the resulting matrix equation is [13],

$$[\,Z\,]\,[\,I'\,] \;=\; [\,V\,] \tag{11}$$

where [Z], [I'] and [V] are known respectively as the generalized impedance matrix, the generalized current vector and the generalized voltage vector. Here, the rough current approximation of Carrel has been avoided by representing the current on each wire segment (*i.e.* only a portion of the dipole) by a second or even a third order polynomial function. Moreover, the mutual impedances are not evaluated here on a pair by pair basis as suggested by Carrel and many other investigators.

We know that the driving voltage sources are only found at the feed points at the base of the dipoles, and that the impressed voltages on all other points on the dipoles are zero. Therefore, by rearranging the generalized impedance matrix [Z] of (11), and the partitioning of this matrix such that the known zero voltages (grouped in vector $[V_b]$), are separated from the known voltage sources (grouped in vector $[V_a]$) in the right hand side of (11), equation (11) yields,

$$\begin{bmatrix} Z_{aa} & Z_{ab} \\ Z_{ba} & Z_{bb} \end{bmatrix} \begin{bmatrix} I_a \\ I_b \end{bmatrix} \;=\; \begin{bmatrix} V_b \\ 0 \end{bmatrix} \tag{12}$$

The entries of the submatrices $[Z_{aa}]$, $[Z_{ab}]$, $[Z_{ba}]$ and $[Z_{bb}]$ are all known, and are in fact entries in matrix Z of (11). Also, the entries of vector $[V_b]$ are all zeros. Therefore, equation (2) can be easily deduced from (12), and hence $[Z_a]$ is found to be [14],

$$[\,Z_a\,] \;=\; [\,Z_{aa}\,] - [\,Z_{ab}\,]\,[\,Z_{bb}\,]^{-1}\;[\,Z_{ba}\,] \tag{13}$$

This means that a smaller square matrix $[Z_a]$ of order N is formed by little numerical manipulation on the elements of the generalized impedance matrix.

Now by solving equation (7), the base voltage vector $[V_a]$ is found and hence the right hand side of (12) is known. Equation (12) is, thus, solved for the current distribution on the dipoles. The determination of this current distribution is the principal and most difficult task in any radiation problem. Once, this is found, it is a relatively simple matter to determine the distant far field, the gain, the input impedance and any other radiation characteristics required.

Numerical Results

In order to evaluate the confidence given by the present approach, verify the results of the calculations, and ascertain the accuracy obtainable with the method presented here, several problems are solved and compared with other results available in the literature. Based on the above equations, a digital computer program, written in FORTRAN and run on the Digital Equipment Corporation VAX 11/785 computer, is developed in order to analyse the LPDA of any given structural bandwidth. The LPDA is solved here for the current distribution, far field pattern, gain, standing wave ratio (SWR), and input impedance.

The LPDA is solved for the two sets of parameters, given in Table 1, so as to allow the comparison with the experimental results of DeVito and Stracca [4]. Fig. 3 shows the normalised H-plane radiation patterns ($E_\theta \rightarrow \phi$) of both our numerical results and their experimental results. Curves (a) are for LPDA # 1 and curves (b) for LPDA # 2. Very close agreement is shown for both antennas. In Fig. 4, the normalized magnitude and the phase of the base current of each dipole element are shown at three different frequencies. Only those elements of the radiating region are excited. It is apparent that as the frequency increases, the element of maximum current moves from a longer dipole to a shorter one, *i.e.* the active region moves towards shorter elements. More comparison is also made but with the theoretical results of DeVito and Stracca [4]. Fig. 5 shows the curves of the gain calculated by them and those computed by the present approach. The gain is plotted vs. the spacing factor σ for different values of τ (0.82, 0.86, 0.96). Close agreement is shown for $\tau = 0.86$, and fair agreement for $\tau = 0.82$. However, for $\tau = 0.96$, a difference of about 1 dB at $\sigma = 0.1$ is shown and increases as σ increases to reach about 3 dB at $\sigma = 0.2$. This discrepancy may be referred to the inaccurate current distribution considered by DeVito

Table 1.

Parameters	LPDA # 1	LPDA # 2
$Z_T = Z_f(\Omega)$	100	420
τ	0.8	0.93
σ	0.14	0.146
N (dipoles)	12	12
Freq. of Test (MHz)	780	480
$\frac{l_N \text{ (mm)}}{l_1 \text{ (mm)}}$	26.5 308	151 336
h/a	125	125
Length of LPDA (mm)	395	84

and Stracca, which does not have much effect in the calculation of the H-plane pattern, but has considerable effect on the gain.

A third comparison is made with Kyle [7]. The directivity is computed against frequency for the following LPDA parameters, $\tau = 0.92$, $\sigma = 0.12$, N = 12 dipoles, h/a = 118, $Z_f = 104\ \Omega$ and $Z_T = 0$ (*i.e.* short circuit termination), with an external transmission line characteristic impedance of 73Ω. The starting frequency being 635 MHz. The discrepancy shown in Fig. 6, is due to Kyle's results who evaluated the mutual impedances on a pair by pair basis as employed by Carrel.

Design Considerations

From the above comparisons, greater confidence can be put on the present approach. Three sets of curves, useful to antenna designers, are thus computed and

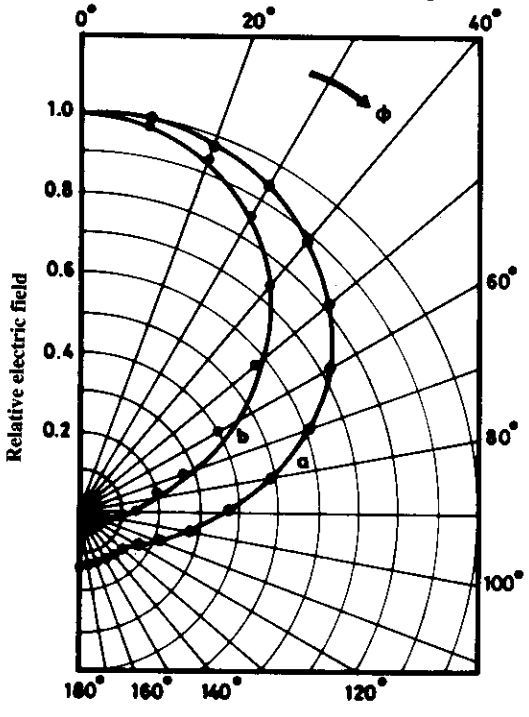

Fig. 3. Normalised H-plane Radiation Pattern E_θ vs. ϕ
Curve a: τ= 0.8, σ=0.14, Z_f = 100Ω, h/a = 125, $Z_T = Z_f$
Curve b: τ= 0.93, σ=0.146, Z_f = 420Ω, h/a = 125, $Z_T = Z_f$.
●●● : DeVito and Stracca [4]
——— : This method

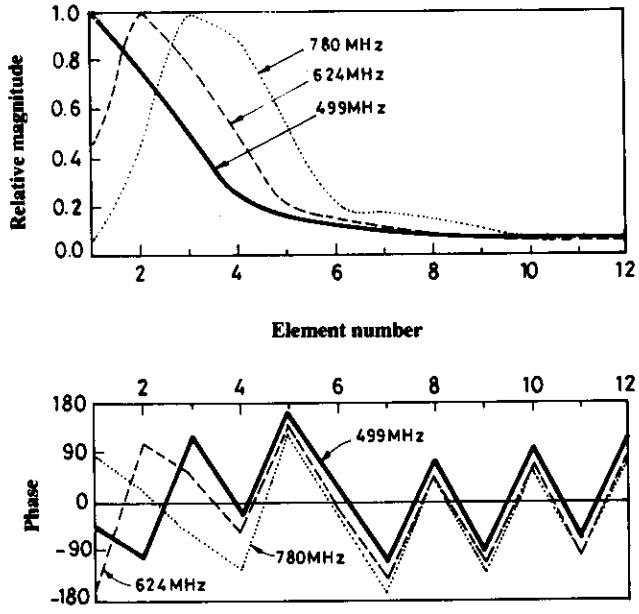

Fig. 4. Current magnitude and phase at the base of the LPDA dipole elements for three frequencies within the operating bandwidth. $\tau = 0.8$, $\sigma = 0.14$, $Z_f = 100\Omega$, $h/a = 125$, $Z_T = Z_f$

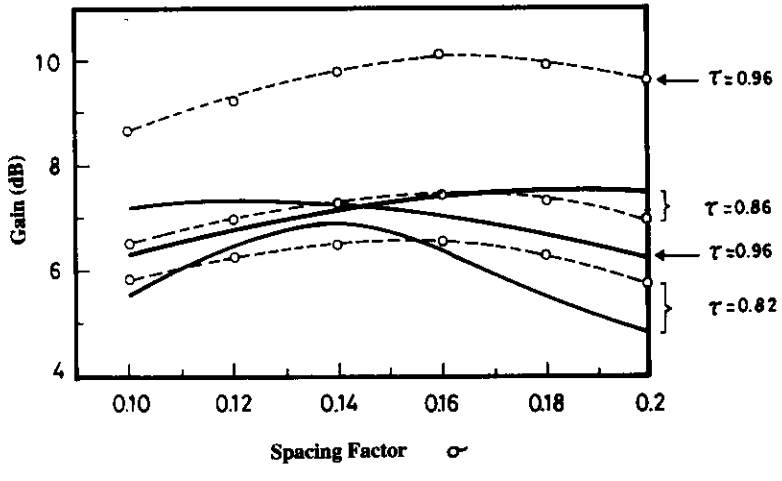

Fig. 5. Gain vs. σ for different values of τ ($Z_f = Z_T = 100$, $h/a = 125$m, $N = 8$)
.. o ..: DeVito and Stracca [4]
——— : This method

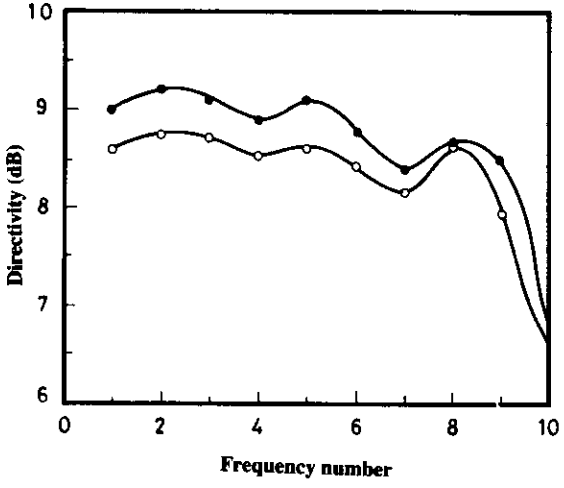

Fig. 6. Directivity vs. frequency for the LPDA when $\tau = 0.92$, $\sigma = 0.12$, N = 12, h/a = 118, $Z_f = 104\Omega$, Z_T = short circuit, External transmission line impedance = 73Ω, f_1 = 635 MHz.
—o— : Kyle [7]
—●— : This method

illustrated in Figs. 7, 8 and 9. These are, respectively, for the gain, SWR and input resistance vs. the feeder characteristic impedance Z_f for different values of τ (0.82, 0.88, 0.96) at each and every value of σ (0.1, 0.14, 0.18). The LPDA, used to calculate these design curves, has N = 8 dipoles, h/a = 125, and the large end termination is equal to the feeder characteristic impedance, *i.e.* $Z_T = Z_f$. The starting frequency is taken to be 480 MHz. When $\tau = 0.96$, each dipole is modeled with two segments, while it is modeled with four segments for $\tau = 0.88$ and $= 0.82$. The currents on the segments are approximated by second order polynomials in the 1st and 2nd cases, and by third order polynomials in the last case. This is because as τ decreases, the structural bandwidth is larger for a given number of dipoles, and the largest dipole becomes longer and longer in terms of wavelength at the highest frequency of operation, which requires dividing the dipoles into more segments, using higher order current approximations, or both.

The useful bandwidth of the antenna depends on the distance the active region can move before it includes the smallest or largest element, and hence before the antenna properties become distorted. Therefore, the useful bandwidth B, over which the antenna properties are almost constant, is always less than the structural bandwidth B_s. Unfortunately, there is no clearcut identification for the useful bandwidth. Here, the curves of Figs. 7, 8 and 9 are plotted by taking the average

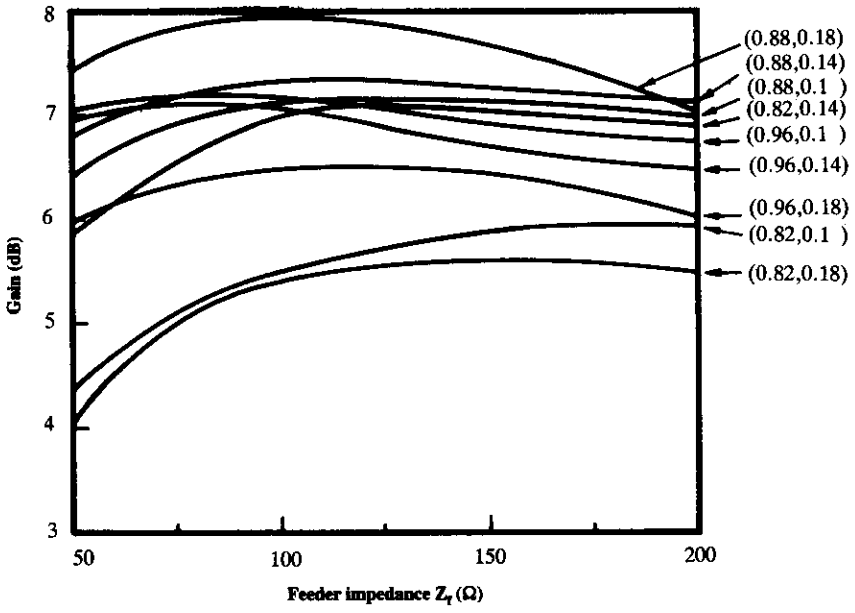

Fig. 7. Gain vs. feeder impedance for different values of τ (0.82, 0.88, 0.96) at the following values of σ (0.1, 0.14, 0.18). The values of τ and σ are shown respectively beside each curve.

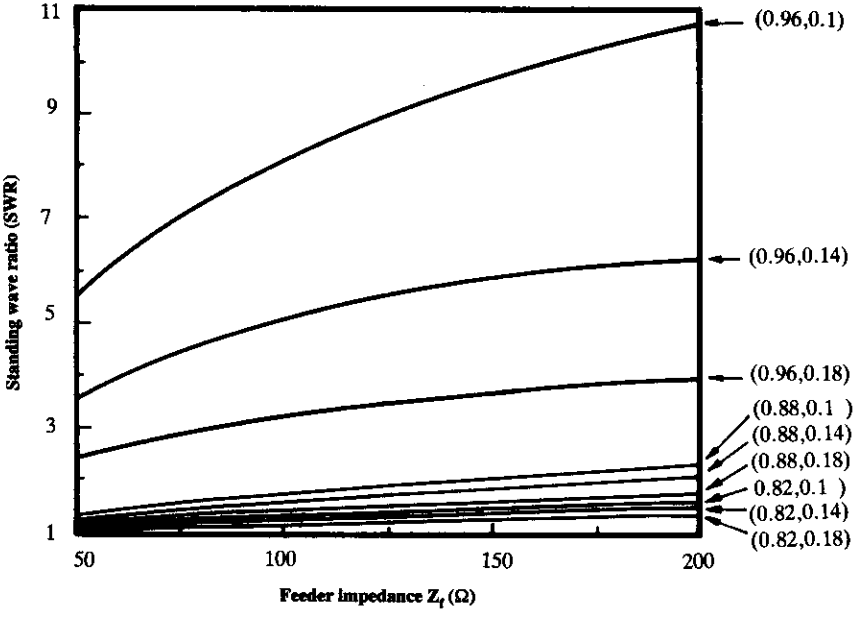

Fig. 8. Standing wave ratio vs. feeder impedance for different values of τ (0.82, 0.88, 0.96) at the following values of σ (0.1, 0.14, 0.18). The values of τ and σ are shown respectively beside each curve.

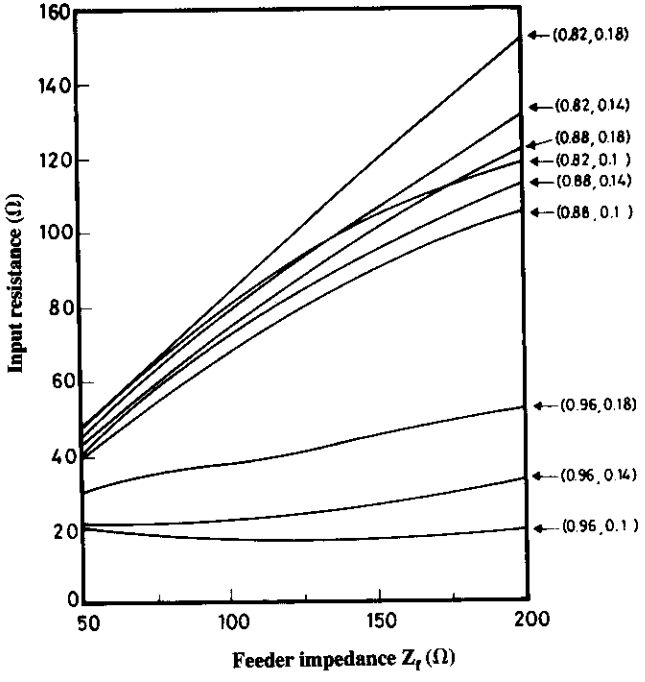

Fig. 9. Input resistance vs. feeder impedance for different values of τ(0.82, 0.88, 0.96) at the following values of σ (0.1, 0.14, 0.18). The values of τ and σ are shown respectively beside each curve.

value over the six operating frequencies at which the 6 middle dipoles are resonating. That is the values at the resonance frequencies of the largest and smallest dipoles are excluded from our calculations. In other words, the useful bandwidth is taken to be l_2/l_{N-1}.

In Fig. 7 as Z_f increases the gain increases and approaches a maximum value when the characteristic impedance of the transmission line is 100Ω. and then it starts decreasing. This behavior is not well noticed for lower values of τ. It is seen at higher values of τ (τ= 0.96) but the gain is not the highest. Maximum gain can be obtained when τ is around 0.88 and at the highest value of σ (σ = 0.18).

In Fig. 8, the SWR is almost insensitive to the variation of Z_f, especially for lower values of τ and as σ increases. In other words, the larger the value of τ and the lower the value of σ, the larger the variation of SWR with Z_f. For low SWR, τ must also be lower and σ must be higher. This means that by covering the frequency band with fewer dipoles and increased spacings, matching of the LPDA is improved.

In Fig. 9, with τ fixed, the increase in σ (*i.e.* the increase of spacings between elements) results in an increase in the input resistance. Similarly, with fixed σ, the input resistance increases as τ decreases. However, the input resistance becomes insensitive to the variation of Z_f for higher values of τ and lower values of σ, *i.e.* as the structural bandwidth is smaller and the antenna becomes more compacted. Also, for lower values of Z_f, the input resistance approaches more the characteristic impedance of the feeder than at higher values of Z_f, and as τ decreases and σ increases. This means that matching is obtained for lower τ and higher σ and at a lower value of Z_f.

Therefore, for the LPDA under consideration, one can deduce from the above discussion and Figs. 7, 8 and 9, that for a higher gain, lower SWR and in order to be close to the matching condition, the characteristic impedance of the transmission line feeder must be around $Z_f = 100\Omega$, and τ and σ must be around 0.88 and 0.18 respectively as the best compromise among them. These steps may also be followed for the design of any other LPDA.

Conclusions

The dipole array circuit of the log-periodic dipole antenna is solved by the numerical Bubnov Galerkin's technique to give the current distribution on the dipoles. The far field, gain, directivity, input impedance and standing wave ratio are then calculated and compared with other results available in the literature. Results have proven the suitability of the present approach. Also, many curves are plotted for different values of τ, σ and Z_f. These curves can be used in the design of the LPDA by deducing the values of the parameters, τ, σ and Z_f at which good results can be achieved. For σ less than about 0.05, the dipoles are close together, causing some difficulty in performing the integrations of the generalised impedance matrix.

Assuming symmetry, and considering continuity of the current at the wire joints, the calculation time of the generalized impedance matrix elements is reduced by about half. Since most of the computation time is spent in the calculation of such elements, computation is further decreased by storing some of them to use at the next frequency. Typical CPU time on VAX 11/785, which is about ten times slower than the IBM 3083, is around five minutes for a twelve dipole array, at twelve frequencies, and when each dipole is split into 4 wire segments with the current on each approximated by a third order polynomial. The method has been tested successfully and applied to several LPDA array operating over different bandwidths and for different values of τ and σ.

References

[1] Isbell, D.E. "Log-periodic Dipole Arrays." *IRE Trans. Antennas Propagat.*, AP-8, May (1960), pp. 260-267.

[2] Carrel, R.L. "The Design of Log-periodic Dipole Antennas." *The 1961 IRE Int. Convention Record*, Vol. I, (1961), pp. 61-75.

[3] Cheong, W.M. and King, R.W.P. "Log-periodic Dipole Antenna." *Radio Sci.*, 2, Nov. (1967), 1315-1326.

[4] DeVito, G. and Stracca, G.B. "Comments on the Design of Log-periodic Dipole Antennas." *IEEE Trans. Antennas Propagat.*, AP-21, May (1973), pp.303-308.

[5] Cheong, W.M. and King, R.W.P. "Arrays of Unequal and Unequally Spaced Elements." *Radio Sci.*, 2, Nov. (1967), 1303-1314.

[6] DeVito, G. and Stracca, G.B. "Further Comments on the Design of Log-periodic Dipole Antennas." *IEEE Trans. Antennas Propagat.*, AP-22, Sept. (1974), pp. 714-718.

[7] Kyle, R.H. "Mutual Coupling between Log-periodic Antennas." *IEEE Trans. Antennas Propagat.*, AP-18, Jan.(1970), pp.15-22.

[8] Harrington, R.F. *Field Computation by Moment Methods*. New York: The MacMillan Company, 1968.

[9] Sinnott, D.H. "Multiple-frequency Computer Analysis of the Log-periodic Dipole Antenna." *IEEE Trans. Antennas Propagat.*, AP-22, July (1974), pp. 592-594.

[10] Gong, Z.L. and Balmain, K.G. "Reduction of the Anomalous Resonances of Symmetric Log-periodic Dipole Antennas." *IEEE Trans. Antennas Propagat.*, AP-34, Dec. (1986), pp. 1404-1410.

[11] Campbell, C.K.; Traboulay, I.; Suthers, M.S. and Kneve, H. "Design of a Stripline Log-periodic Dipole Antenna." *IEEE Trans. Antennas Propagat.*, AP-25, Sept. (1977), pp.718-721.

[12] Pantoja, R.R.; Sapienza, A.R. and Filho, F.C. "A Microwave Printed Planar Log-periodic Dipole Array Antenna." *IEEE Trans. Antennas Propagat.*, AP-35, Oct. (1987), pp. 1176-1178.

[13] Hassan, M.A.; Silvester, P.; Howarth, B. and Nasu, N. "Solution to the Interconnected Wire Scatterer Problem." *Proc. IEE*, Vol. 123 (1976), pp.509-514.

[14] Chan, K.K. and Silvester, P. "Analysis of the Log- periodic V-dipole Antenna." *IEEE Trans. Antennas Propagat.* AP-23, May (1975), pp. 397-401.

Appendix

Determination of (9)

Consider the two wire segments m and n whose current directions $\hat{m}$ and $\hat{n}$ are similarly oriented in the $\hat{z}$ direction as shown in Fig. A. They are located on two different LPDA dipoles. The tangential electric field E_{tan} at the field point $s_n(y', z')$ on the surface of segment n due to a source point s_m on the axis of segment m is given by:

$$E_{tan} = \overline{E}(s_n).\hat{n} = E_z(s_n) = -j\omega\mu A_z + \frac{1}{j\omega\varepsilon}\frac{\partial^2 A_z}{\partial z'^2} \qquad (A.1)$$

where

$$A_z(s_n) = \int_0^{l_m} I^m(s_m)\frac{\exp(-jkR_{mn})}{4\pi R_{mn}}\, ds_m \qquad (A.2)$$

is the magnetic vector potential at s_n due to the current $I^m(s_m)$ flowing in segment m, and

$$R_{mn} = [\, y'^2 + (z' - s_m)^2 + a_n^2 \,]^{\frac{1}{2}} \tag{A.3}$$

is the distance between the source and field points. ω, μ and ϵ are respectively the radian frequency, the permeability and the permitivity. k is 2π/wavelength. a_n is the radius of segment n. If A_z is given by (A.2), then

$$\frac{\partial A_z}{\partial z'} = \int_0^{l_m} I^m(s_m) \frac{\exp(-jkR_{mn})\,(z' - s_m)\,(-1 - jkR_{mn})}{4\pi R_{mn}^3}\, ds_m \tag{A.4}$$

and

$$\frac{\partial^2 A_z}{\partial z'^2} = \int_0^{l_m} I^m(s_m) \frac{\exp(-jkR_{mn})}{4\pi R_{mn}^5} \{-(1+jkR_{mn})\,R_{mn}^2 - k^2 R_{mn}^2 (z' - s_m)^2 + 3(1+jkR_{mn})\,(z' - s_m)^2\}\, ds_m \tag{A.5}$$

substituting (A.2) and (A.5) into (A.1) and knowing that $-j\omega\mu$ is equal to $k^2/j\omega\epsilon$, we obtain

$$E_{tan} = \frac{1}{j\omega\epsilon\, 4\pi} \int_0^{l_m} I^m(s_m)\, F(s_n, s_m)\, ds_m \tag{A.6}$$

where,

$$F(s_n, s_m) = \frac{\exp(-jkR_{nm})}{R_{nm}^5} \{\, R_{nm}^2 (-1 - jkR_{nm} + k^2 R_{nm}^2) + (z' - s_m)^2 (3 + 3jkR_{nm} - k^2 R_{nm}^2) \,\} \tag{A.7}$$

Now, if the segment end (y_m, z_m) of segment m is not located at the origin, therefore the vertical distance $(z' - s_m)$ given in (A.7) becomes $(z_n + s_n - z_m - s_m)$, and the distance R_{mn} between the source and field points yields,

$$R_{mn} = (y_n - y_m)^2 + (z_n + s_n - z_m - s_m)^2 + a_n^2 \tag{A.8}$$

Also, note that if the segment currents are in opposite directions (*i.e.* $\hat{m}.\,\hat{n} = -1$), then the RHS of (A.1) and hence of (A.6) will be multiplied by –1, or $F(s_n, s_m)$ of (A.7) is negated.

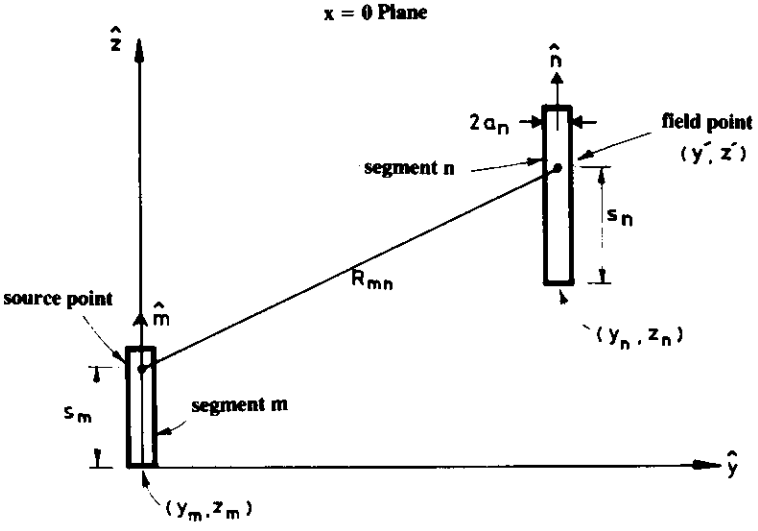

Fig. A. Two wire segments on two different LPDA dipoles

طريقة تحليل رقمية للهوائي ثنائي القطبية اللوغاريتمي

محمد عبدالعزيز حسن

قسم الهندسة الكهربائية، كلية الهندسة، جامعة الملك سعود، ص.ب ٨٠٠، الرياض ١١٤٢١، المملكة العربية السعودية

ملخص البحث. نقدم في هذا البحث طريقة رقمية لتحليل مصفوفة من الهوائيات ثنائية القطبية اللوغاريتمية. وقد اعتبرت مصفوفة الهوائيات هذه كدائرتين كهربائيتين منفصلتين، هما دائرة الهوائيات ودائرة خط النقل المغذي للهوائيات. ولقد عولجت الهوائيات كمسألة قيمة حدية ممثلة بمجموعة من المعادلات التكاملية. ومن ثم تم حل هذه المعادلات بطريقة بابنوف جالاركن باستخدام كثيرات حدود لاجرانج كدوال أساسية. وتسمح هذه الطريقة بتقويم كامل ودقيق لعمل هذا النوع من الهوائيات في أي نطاق ترددي مطلوب ولأي بارامترات تصميم معطاة. وفي هذا البحث تم رسم منحنيات كثيرة عند قيم مختلفة للبارامترات من أجل إيجاد أفضل قيم تصميم لها. وبمقارنة النتائج التي حصلنا عليها وجدناها تتفق ونتائج الطرق الأخرى السابق نشرها.